Blind source identification from the multichannel surface electromyogram

2014 Physiol. Meas. 35 R143

(http://iopscience.iop.org/0967-3334/35/7/R143)

IOP Publishing | Institute of Physics and Engineering in Medicine Physiological Measurement

Physiol. Meas. **35** (2014) R143–R165 doi:10.1088/0967-3334/35/7/R143

Topical Review

Blind source identification from the multichannel surface electromyogram

A Holobar[1] **and D Farina**[2]

[1] System Software Laboratory, Institute of Computer Science, Faculty of Electrical Engineering and Computer Science, University of Maribor, Maribor 2000, Slovenia
[2] Department of Neurorehabilitation Engineering, Bernstein Center for Computational Neuroscience, Bernstein Focus Neurotechnology Göttingen, University Medical Center Göttingen, Georg-August University, D-37075 Göttingen, Germany

E-mail: ales.holobar@um.si

Received 18 November 2013, revised 23 April 2014
Accepted for publication 23 May 2014
Published 19 June 2014

Abstract

The spinal circuitries combine the information flow from the supraspinal centers with the afferent input to generate the neural codes that drive the human skeletal muscles. The muscles transform the neural drive they receive from alpha motor neurons into motor unit action potentials (electrical activity) and force. Thus, the output of the spinal cord circuitries can be examined noninvasively by measuring the electrical activity of skeletal muscles at the surface of the skin i.e. the surface electromyogram (EMG). The recorded multi-muscle EMG activity pattern is generated by mixing processes of neural sources that need to be identified from the recorded signals themselves, with minimal or no *a priori* information available. Recently, multichannel source separation techniques that rely minimally on *a priori* knowledge of the mixing process have been developed and successfully applied to surface EMG. They act at different scales of information extraction to identify: (a) the activation signals shared by synergistic skeletal muscles, (b) the specific neural activation of individual muscles, separating it from that of nearby muscles i.e. from crosstalk, and (c) the spike trains of the active motor neurons. This review discusses the assumptions made by these methods, the challenges and limitations, as well as examples of their current applications.

Keywords: surface EMG, factorization, decomposition, muscle synergies, activation primitives, neural drive to muscles, motor unit

(Some figures may appear in colour only in the online journal)

1. Introduction

Human movements result from the neural activity of cells in the central (CNS) and peripheral (PNS) nervous systems and the ultimate transformation of the neural code into muscle forces. These mechanisms are still not fully understood because of the complexity of neural interactions that are difficult to measure *in vivo*. In the CNS, millions of neurons mutually interact for the generation of motor commands, interchanging information in the form of electrical pulses. In the PNS, the number of motor neurons involved in the generation of a motor command is in the order of several hundreds (Gosselin 2011, Hannan *et al* 2012). These numbers present important challenges to current neural interfacing methods, which typically record from either too few or too many cells for an effective interpretation of the neural signal.

When analyzing human motor functions, the neural code associated with the output layers of the spinal cord circuitries can be examined by measuring the electrical activity of skeletal muscles, the so called electromyogram (EMG). The EMG reflects the activity of alpha motor neurons (see section 2), thus providing an insight into the final output of the neuromuscular system i.e. into the neural commands sent to the muscles. With respect to a direct measure from efferent peripheral nerve fibers, the muscle signals spatially spread the information from the PNS, significantly decreasing the number of physiological sources per unit volume. This simplifies the design of uptake electrodes that can be larger and less selective than the neural ones, while still providing the same level of information on the neural activation. Moreover, because the electrical activity of a single motor neuron is projected to several tens or hundreds of muscle fibers (section 2), muscles electrically amplify the activity of motor neurons. This amplification is so efficient and robust that it warrants the sampling of the neural activation non-invasively with surface EMG (Merletti and Parker 2004, Merletti *et al* 2010).

The information extracted from the surface EMG is used e.g. in pathophysiological investigations and diagnostic systems (Ling *et al* 2007, Minetto *et al* 2007, Sanger 2008, Zhang *et al* 2013, Zhang *et al* 2011, Watanabe *et al* 2012, Vaiman and Krakovski 2012, Woźniak *et al* 2013, Neblett *et al* 2013, Meigal *et al* 2013), and as a basis for man–machine interfacing, especially for the control of active prostheses/orthoses (Evans *et al* 1984, Jiang *et al* 2009, 2012, Kuiken *et al* 2009, Lorrain *et al* 2011, Muceli and Farina 2012, Pantall *et al* 2011, Richard *et al* 1983). The challenge in these applications is the identification of the neural mechanisms underlying the observed muscle activity.

Motor neurons are the final common pathways of the neuromuscular system and combine their synaptic input to determine the final neural drive to muscles (figure 1). Therefore, the surface EMG, as a measure of the output motor neuron spike trains, contains information on both central and peripheral neural mechanisms for movement generation. However, sources of neural information are superimposed at different levels (figure 1) and in mixing processes that are largely unknown and, as such, need to be estimated from each individual EMG recording (Djuwari *et al* 2006, Holobar *et al* 2009). The extraction of information from the surface EMG is, thus, a challenge of source separation that must be addressed at various scales. Sources in the EMG can be viewed as the high-level commands that generate a movement, or as the neural activation to each individual muscle and muscle compartment, or, eventually, as the activation of the individual smallest functional units of movement i.e. the motor units (MUs). Depending on the signal model at the scale of interest, the observed EMG signals can be viewed as linear instantaneous or convolutive mixtures of the sources (see section 2). In the former case, the sources are linearly combined for each time sample with scalar weights. In the latter, the sources are filtered by unknown linear filters before being mutually superimposed to obtain the observations.

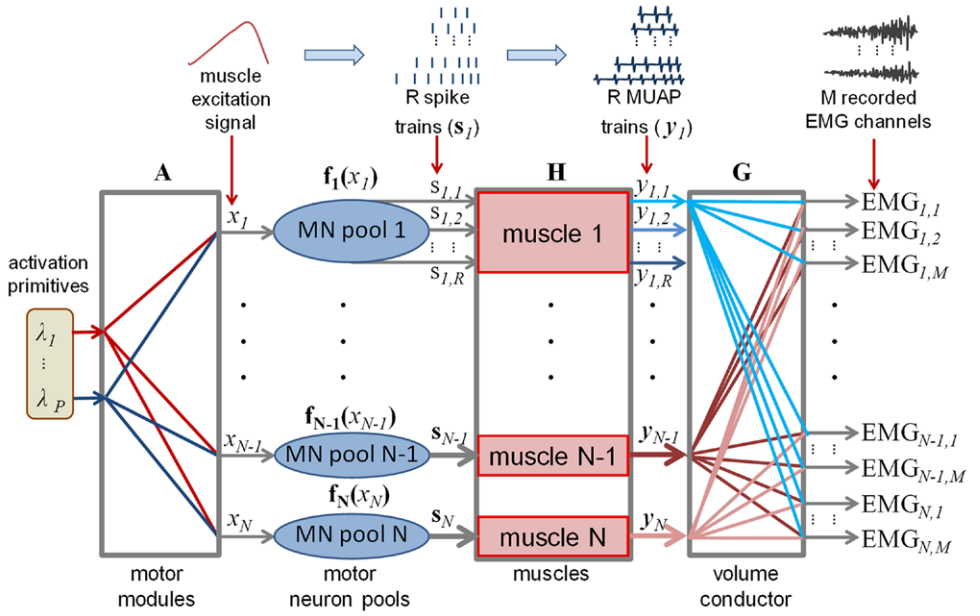

Figure 1. The multi-scale model of movement generation proposed in this review. From left to right: P activation primitives are shared by N motor neuron pools ($P < N$). Each motor neuron pool receives the linear combination of the P activation primitives as input and transforms this input into spike trains that drive the innervated muscle (thus, the scheme presents N muscles). The N muscles contribute to M ($M > N$) EMG channels by the trains of motor unit action potentials. According to this scheme, the neural commands are first mixed by the synergy matrix **A**, then undergo nonlinear transformations at the level of the motor neuron pools, and are finally mixed again by the volume conductor matrices **H** and **G**. The muscle transformation is represented by a matrix **H** that corresponds to the generation of action potential trains from the motor neuron spike trains. As discussed in what follows, **A** is usually assumed to be a scalar matrix and the corresponding mixture as a linear instantaneous mixture. **G** may represent either a convolutive or an instantaneous mixing process. Indeed, the transformation between motor unit action potential trains and muscle channels implies, in the most general case, that each action potential train contributes to all EMG channels, being filtered by a train-specific and channel-specific filter. When crosstalk between muscles is assumed to be linear, the matrix **G** is a matrix of scalars. At the higher level, the P activation primitives are estimated from NM EMG channels (M channels for each muscle) to extract supraspinal command signals underlying movement generation. In this case, it may be relevant to separate true muscle activation from crosstalk i.e. to solve the mixing corresponding to the matrix **G** and thus to estimate the sum of the R motor unit action potential trains for each muscle. At the finest level, the set of motor neuron spike trains $\mathbf{s}_i$ is estimated for each muscle from the recorded M EMG channels per muscle.

Source separation methods have been developed to exploit the full aforementioned range of information from the surface EMG. From the coordinated activity of multiple muscles, sources have been extracted as the signals underlying the complex muscle activation patterns (Djuwari *et al* 2006, Gizzi *et al* 2011, 2012, Muceli *et al* 2010, Roh *et al* 2012, Sartori *et al* 2013, Ting and Macpherson 2005, Torres-Oviedo and Ting 2010, Zariffa *et al* 2012). At a smaller scale, the EMG has been processed to identify the activity of the target muscle (or muscle compartment) and separate it from that of nearby muscles (De Luca and Merletti 1988, Farina *et al* 2004a, Farina *et al* 2008, Jensen *et al* 2013, Léouffre *et al* 2013, Staudenmann *et al* 2007, Naik and Kumar 2012, Naik *et al* 2011, Naik *et al* 2008). Finally, at the individual muscle level, the individual MUs have been identified from the interferential EMG (Holobar

and Zazula 2004, Holobar and Zazula 2007a, Holobar *et al* 2009, 2010, 2012, De Luca *et al* 1982, 2006, Nawab *et al* 2010).

In this review, we focus on the methods for source identification from the surface EMG at the various scales described. We limit our focus to the so called blind source separation techniques that implicitly combine the information from multiple uptake electrodes with minimal or no *a priori* information. In the last decade, these methods have been extensively tested (Holobar and Zazula 2004, Holobar and Zazula 2007a, Holobar *et al* 2009, 2010, 2012, 2014, Marateb *et al* 2011) and have demonstrated potential for a vast range of applications that will be briefly discussed with representative examples.

2. Signal modeling

2.1. Signal generation

It would be computationally very expensive for the CNS to control each muscle individually (Bernstein 1967). Rather, a long lasting hypothesis is that the CNS adopts strategies that can simplify the control by modularity i.e. by combining a small number of behavioral units. Accordingly, a modular organization of motor behavior has been observed in frog limb movements (D'Avella *et al* 2003), in cat postural responses (Torres-Oviedo *et al* 2006), in primate grasping (Overduin *et al* 2008), and in human reaching (D'Avella *et al* 2006, Muceli *et al* 2010), walking (Gizzi *et al* 2011, Ivanenko *et al* 2004), and pedaling (Raasch and Zajac 1999). According to this scheme, the multi-dimensional muscle patterns, as measured by the EMG signal, are generated as a linear combination of a smaller number of signals, which are task-related (figure 1).

When looking at a smaller scale, corresponding to the activity of individual muscles or muscle compartments, the electrical activity recorded in a spatial location as EMG is the mixture of the activity of many concurrently active muscle compartments and nearby muscles (figure 1). This phenomenon is known as EMG crosstalk (De Luca and Merletti 1988) and intrinsically limits our possibility to measure the neural activation in single muscles.

Finally, the EMG activity of each muscle can be studied at the level of individual MUs (De Luca *et al* 1982, Holobar and Zazula 2004, Holobar *et al* 2009, Nawab *et al* 2010), which are the smallest functional sources in a movement. The information extracted on this scale maps directly to the activity of alpha motor neurons and provides a definitive insight into the net output from the CNS and PNS (Farina *et al* 2010). Both motor neuron axons and muscle fibers implement the 'all-or-nothing' principle of electrical activation. Thus, in the time domain, their activity can be modeled by spike trains i.e. binary sequences of zeros and ones, with ones indicating a discharge and zeros standing for the periods with no discharges (Holobar *et al* 2007a, 2009). Due to the intrinsic properties of the neuromuscular system (Merletti and Parker 2004), these spike trains are sparse, so that each spike is followed by a series of several zeros. In normal conditions, the neuromuscular junction is highly stable, so that every spike in the motor neuron triggers the electrical activation of the innervated muscle fibers to generate single fiber action potentials (SFAP).

The compound action potential of all the fibers innervated by a motor neuron is known as motor unit action potential (MUAP). MUAPs are function of space (figure 2) and their shapes reflect the muscle properties (e.g. the conduction velocity of the action potentials), volume conductor characteristics (e.g. conductivity of the interposed tissue), and the acquisition system properties (e.g. the size of an uptake electrode area). Therefore, the shapes of MUAPs are largely unknown *a priori* and vary with conditions, such as the subject anatomy,

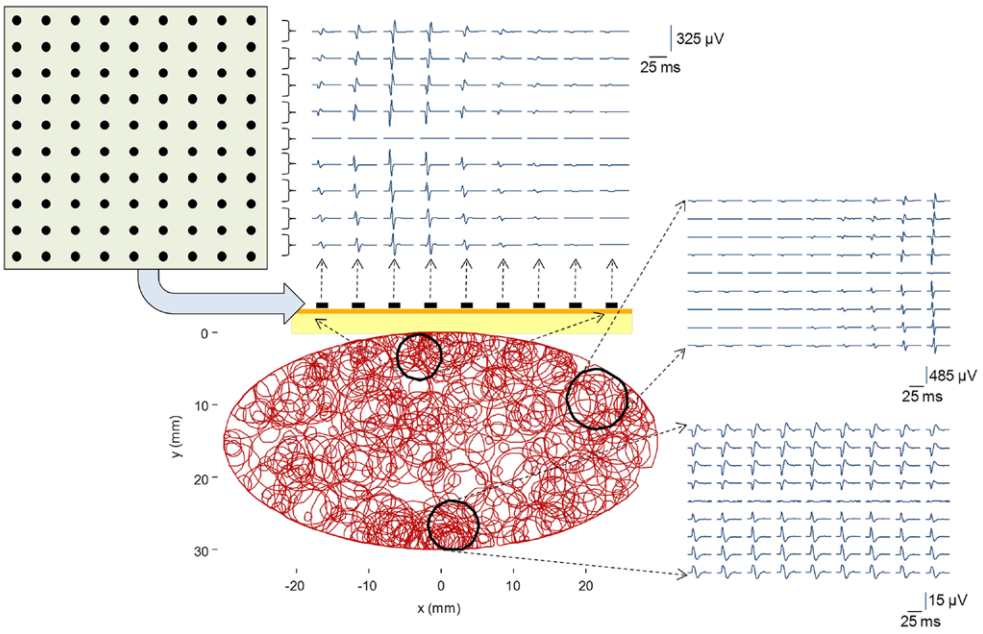

Figure 2. Simulated motor unit territories in a muscle cross-section (center) and multichannel MUAPs of three spatially distinct MUs, as detected by a grid of 10×9 surface electrodes (5-mm interelectrode distance in both directions) in bipolar configuration. The grid of electrodes is schematically depicted in the upper left corner. MUAPs were generated by the volume conductor model described in Farina *et al* (2004c).

spatial distribution of the muscle fibers within the muscle, and fatigue (Blok *et al* 2005, Farina *et al* 2002, 2004b, Farina and Merletti 2001, Farina and Rainoldi 1999, Roeleveld *et al* 1997a, 1997b). Moreover, in dynamic contractions, the action potential shapes may change rapidly over time due to the continuous variation of the relative position of the electrodes with respect to the muscle fibers.

By combining several SFAPs into one MUAP, the MUs, and thus muscles, can be seen as natural amplifiers of the neural code conducted by motor neurons, with the amplitude gain typically exceeding the factor of several tens. Thus, when compared to electrical recordings of a nerve, the recording of MU electrical activity is less technologically demanding and can be made non-invasively by using surface EMG electrodes (Merletti *et al* 2010). The latter detect the activity of a large number of MUs (up to several tens) whose contributions mutually interfere and form a highly complex signal pattern that is difficult to interpret (figure 3). However, multiple surface electrodes can be arranged in two-dimensional arrays (figure 2) in order to exploit the information on spatial variability of the detected MUAPs and decompose the surface EMG into contributions of individual MUs (Holobar and Zazula 2007a).

In a normal and not fatigued condition, MUs discharge with a relatively small degree of synchronicity, so the spike trains are relatively independent. This proves beneficial when the decomposition of multichannel EMG is attempted by the so called independent component analysis (ICA) techniques (Cichocki and Amari 2002, Hyvärinen *et al* 2001) (see section 3 for details). With fatigue and in neurodegenerative disorders, such as Parkinson's disease, the discharges of different motor neurons tend to synchronize, causing either physiological or pathological tremor (Benito-León and Louis 2006, Brittain and Brown 2013).

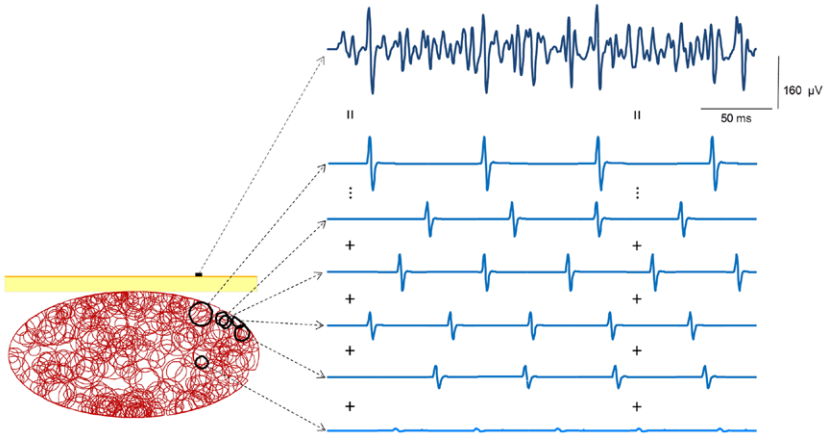

Figure 3. Synthetic surface EMG (top trace) as the sum of individual MUAP trains (bottom traces). Five hundred MUs of different sizes were simulated, with their territories randomly distributed within the simulated elliptical muscle cross-section. Each MU discharged between 8 and 35 MUAPs s^{-1}. For clarity, MUAP trains of only six out of 500 MUs that contributed to the simulated EMG signal are depicted.

In these cases, the assumption of independent sources is not valid anymore, rendering the ICA techniques inappropriate for use in EMG decomposition. Noteably, the assumption of sparse spike trains still holds in these conditions.

2.2. Data models of individual motor unit activity

The volume conductor separating the muscle fibers from the recording electrodes acts as a low-pass spatial filter (Lindstrom and Magnusson 1977). The distribution of electrical potential over the skin surface is thus 'blurred' (low-pass filtered) in a way that depends on the distance between the fibers and the electrodes (figure 2) (Farina and Rainoldi 1999). The smallest scale to which we can model the EMG signal is at the MU level. At this scale, the low-pass filtering effect of the volume conductor and, consequently, the spatial variability of MUAPs constituting each EMG channel (figures 2 and 3) has been modeled in the literature either by instantaneous or convolutive data models (figure 4).

The instantaneous data model of the raw EMG is presented in the upper panel of figure 4 and has been proposed as one of the first data approximations in multichannel electrophysiological recordings (Hyvärinen, Karhunen and Oja 2001). It the case of raw (unmodulated) EMG, it assumes that the MUAP trains of a specific MU as detected by different surface electrodes vary only in their amplitude with location. For example, in the upper panel of figure 4, the MUAP train of the *j*th MU (with the territory depicted in black) is multiplied by the scalar factors 0.40, 0.57, 1.25, and 1.17, when measured by electrodes (a), (b), (c) and (d), respectively. Although not completely realistic, this model allows the application of separation techniques for instantaneous mixtures, for which solid solutions exist (Cichocki and Amari 2002, Hyvärinen *et al* 2001, Theis and Garcia 2006).

The convolutive data model (lower panel of figure 4) assumes that MUAP trains of a specific MU, as detected by different uptake electrodes, share only the time instants of the MU discharges, whereas the shape of the detected MUAPs are modeled by the mixing process itself (Holobar and Zazula 2007a, Holobar *et al* 2009). This is very close to the physiological

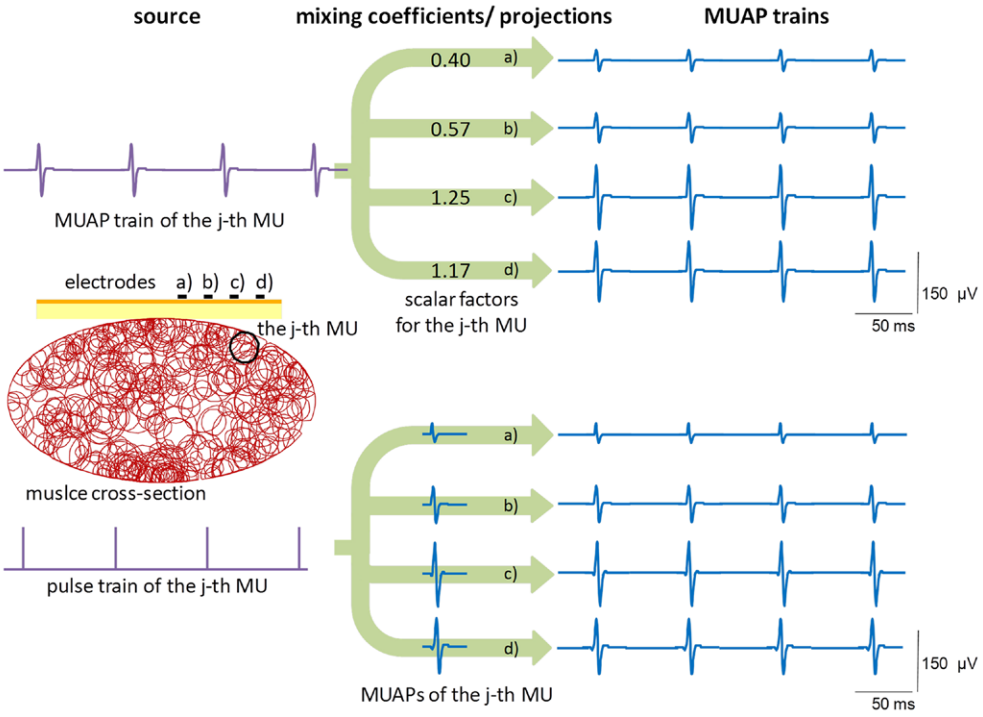

Figure 4. Two data models of MUAP spatial variability. The instantaneous data model (upper panel) assumes that, for each MU, the spatial variability of MUAPs can be modeled by a simple scalar multiplication i.e. by matrix **G** in equation (1). The convolutive data model (lower panel) assumes only that the discharge times of a given MU are shared by different EMG channels whereas the MUAP shapes are modeled as mixing coefficients and can be of arbitrary values, as in equation (3). In the figure, four surface electrodes are schematically depicted and denoted by (a), (b), (c), and (d), but the presented concepts can easily be extended to arbitrary large number of electrodes.

MUAP model and allows for arbitrary spatial variability of MUAP shapes. Thus, the convolutive data model is much more general and realistic than the instantaneous one.

When contributions from several MUs are taken into account, the mixing process of both instantaneous and convolutive model can be modeled by a simple matrix equation (Holobar and Zazula 2007a):

$$\mathbf{EMG}(t) = \mathbf{GH}\bar{\mathbf{s}}(t) + \boldsymbol{\omega}(t) \tag{1}$$

where $\mathbf{EMG}(t)=[EMG_1(t),\ldots, EMG_{NM}(t)]^{\mathrm{T}}$ is a vector of NM unmodulated EMG channels (figure 1), and $\boldsymbol{\omega}(t) = [\omega_1(t), \ldots., \omega_{NM}(t)]^T$ is an additive noise vector.

In the case of instantaneous mixing model, the mixing matrix **H** is block diagonal with the generic MUAP waveforms on the diagonal

$$\mathbf{H} = \begin{bmatrix} MUAP_1(t) & 0 & \cdots & 0 \\ 0 & MUAP_2(t) & \ddots & \vdots \\ \vdots & \vdots & \ddots & 0 \\ 0 & 0 & \cdots & MUAP_{NR}(t) \end{bmatrix}, \tag{2}$$

where $MUAP_j(t)$ denotes the generic MUAP of the jth MU. The $NM \times NR$ matrix **G** comprises the scalar weights describing the MUAP spatial variability (figure 4).

In the case of the convolutive model, **G** contains the volume conductor filters and is, thus, convolutive. In this case, the joint effect of **H** and **G** matrices can be modeled by a matrix that contains the MUAP waveforms from all MUs as detected by all the EMG channels (figure 4):

$$\mathbf{GH} = \begin{bmatrix} MUAP_{1,1}(t) & MUAP_{1,2}(t) & \cdots & MUAP_{1,NR}(t) \\ \vdots & \vdots & \ddots & \vdots \\ MUAP_{NM,1}(t) & MUAP_{NM,2}(t) & \cdots & MUAP_{NM,NR}(t) \end{bmatrix} \quad (3)$$

where $MUAP_{i,j}(t)$ denotes the MUAP of the jth MU as measured by the ith uptake electrode at the time instant t.

In both models, the vector $\bar{\mathbf{s}}(t) = [s_1(t),\ s_1(t-1),\ ...s_1(t-L),\ s_2(t),\ ...,\ s_{NR}(t),\ s_{NR}(t-1)...\ s_{NR}(t-L)]^{\mathrm{T}}$ contains blocks of L consecutive samples from all R motor neuron spike trains in each out of N motor neuron pools (Holobar and Zazula 2007a), where L denotes the sample length of MUAP (without loss of generality, all the MUAPs can be assumed L samples long). As explained in section 2.1, each spike train $s_j(t)$ is modeled as a binary sequence of zeros and ones describing the discharge pattern of the jth motor neuron. Note also that for each muscle, the sources $\mathbf{s}(t)$ are functions of the corresponding muscle excitation signal $x_i(t)$ (figure 1).

Although sparse, the data model (1) is typically undercomplete, with more sources than measurements, and thus difficult to invert (Cichocki and Amari 2002, Hyvärinen *et al* 2001). The number of EMG channels depends on the acquisition system, but is typically limited to several tens. At the same time, there are several tens of MUs active during a motor task, even at low contraction forces. In order to mitigate this problem, the contributions of the MUs with low energy action potentials are typically modeled as physiological noise and embedded into the term $\boldsymbol{\omega}(t)$ in (1). This mathematical trick reduces the number of sources in the data model (1), but also decreases the signal-to-noise ratio (SNR).

When compared to the instantaneous model depicted in figure 4, the convolutive version of the data model increases the number of sources $\mathbf{s}(t)$ by a factor that is proportional to the average sample length of the MUAPs (Holobar and Zazula 2007a, Holobar *et al* 2009). This makes a convolutive model more difficult to invert than the instantaneous counterpart. On the other hand, the instantaneous data model in figure 4 completely ignores the propagation of MUAPs along the muscle fibers and the filtering effect of the volume conductor. Further implications of both data models on MU identification are discussed in section 3.3.

2.3. Data models of EMG crosstalk

When electrodes are placed over a target muscle, whose activity has to be measured, this muscle is not the only contributor and the recorded signals are also influenced by muscles that are nearby (figure 1) (De Luca and Merletti 1988). The greater the distance between the muscle fibers and the uptake electrode, the more attenuated the contribution of this muscle to the electrode (Lindstrom and Magnusson 1977).

Since each MU is associated with a different low-pass filter (figure 2), the mixture of EMG signals from different muscles recorded over a certain location at the surface of the skin cannot be represented as a convolutive mixture of the EMG signals from the individual muscles, but rather as a convolutive mixture of all the action potentials trains of the MUs active in all the nearby muscles (section 2.2). The latter can be modeled as convolutive mixture of the spike trains $\mathbf{s}(t)$ and is defined by equation (1). This approach is the most detailed and general, but is also computationally complex.

In specific conditions, however, the mixture of signals corresponding to crosstalk contributions may be approximated in a simpler way. Specifically, for muscles with small cross-sectional area (compared to the distance from the muscle to the uptake electrodes), the position of all the muscle fibers with respect to all the uptake electrodes is similar. In this case, the EMG signal generated by this muscle can be viewed in the volume conductor as an equivalent source. Moreover, for relative small distances between muscles (which is the case when crosstalk is larger) and small interelectrode distances, the effect of the volume conductor can be approximated as a pure signal attenuation instead of a convolution (Léouffre *et al* 2013). By further neglecting the effect of MUAP propagation along the muscle fibers (i.e. by positioning the linear array of electrodes perpendicular to the muscle fibers), the recorded EMG channels containing the contributions from N active muscles can be modeled as the following instantaneous linear mixture (figure 1):

$$\mathbf{EMG}(t) \approx \mathbf{G}\mathbf{y}(t) = \mathbf{B}\mathbf{D}\mathbf{y}(t), \tag{4}$$

where $\mathbf{G}$ denotes the $NM \times NR$ matrix of crosstalk mixing weights (scalars), $\mathbf{B}$ is a $NM \times N$ matrix and $\mathbf{D}$ is a block diagonal $N \times NR$ matrix with $1 \times R$ blocks of ones on the diagonal. Basically, $\mathbf{D}$ is summing up R MUAP trains from each individual muscle, yielding N muscle contributions.

Note that (4) assumes that the volume conductor filters from all the R MUs of the ith muscle to the jth uptake electrode are equal and can be approximated by a single scalar factor (the (i,j)th element of the matrix $\mathbf{B}$). In this way, it implicitly relies on the instantaneous mixing model of MUAP trains, defined in equations (1) and (2).

The model of linear instantaneous crosstalk (4) has been shown to be valid only within some limits. For example, in Farina *et al* (2004) the blind source separation method based on second order statistics of the measured EMG has been demonstrated to only reduce, not fully eliminate, crosstalk for closely located, and small, forearm muscles. Indeed when considering larger muscles, larger distances or different positioning of electrodes, as described above, the assumption of linear instantaneous mixture for crosstalk is no longer valid (mainly due to the low-pass filtering effect of the volume conductor). Instead, we must separate each muscle signal into the contribution of individual MUs in order to representatively model the EMG crosstalk. In this case, the convolutive mixing process is described by the matrices $\mathbf{G}$ and $\mathbf{H}$ (figure 1). This is further discussed in section 2.4.

2.4. Data models of multi-muscle activity

When EMG signals are detected from multiple muscles, they can be assumed to be an indirect measure of the neural excitation signal sent to each muscle. Because the motor neuron encodes the excitation signal into a rate-coded spike train (figure 1), the extraction of muscle excitation signals is usually performed by demodulating the interference EMG signal i.e. by extracting the low-pass filtered linear envelope or by applying other estimators of signal intensity, such as the average rectified value (ARV) (Clancy and Hogan 1999) or the root-mean-square (RMS) value (Hogan and Mann 1980). Both estimators are frequently used interchangeably, although theoretically the ARV is more appropriate for low-force contractions whereas the RMS is more suitable for high-force contractions (Clancy and Hogan 1999).

The relationship between the net muscle excitation signal and the ARV and RMS value of the EMG is depicted in figure 5. Despite the nonlinear relation between the muscle excitation and the number of MU discharges, the estimated muscle excitation increases approximately linearly with the simulated excitation level. Thus, the ARV and RMS demodulators seem to compensate the nonlinear transformations at the level of the motor neuron pools (for the

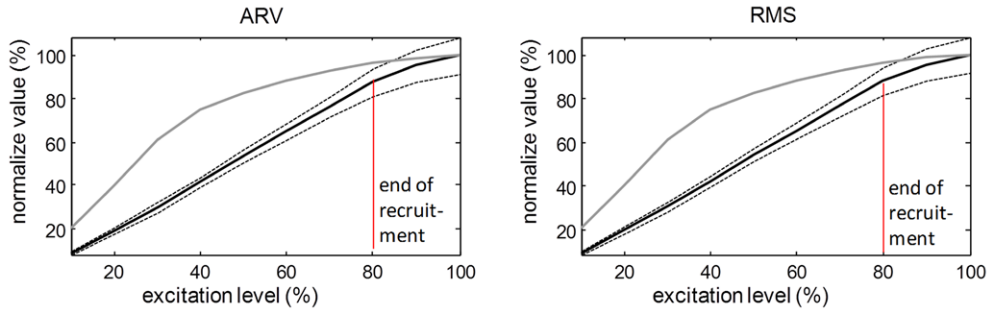

Figure 5. The average rectified value (ARV; left), and root-mean-square value (RMS; right) of the EMG as a function of the muscle excitation. Both demodulators were calculated on a 200 ms long time interval. The total number of MU discharges in the 200 ms time intervals is also depicted (gray thin line). The values are averaged over ten simulation runs, normalized by the values at 100% MVC, and reported as mean values (black solid lines) ± SD (black dashed lines). In each simulation run, the 500 MU were randomly distributed in an elliptical muscle cross-section (see figure 2). The distribution of recruitment thresholds for the motor neurons was modeled with an exponential function with many low-threshold neurons and progressively fewer high-threshold neurons, as described by Fuglevand *et al* (1993). The last MU was recruited at 80% MVC. The discharge rate of simulated MUs increased linearly with the excitation (0.3 pps/%) from 8 to 35 pps. The end of recruitment, after which only rate coding was used to increase muscle force, is indicated by the red vertical bar.

analysis of the motor neuron pool transformation, see Farina *et al* (2013), Farina and Negro (2012), and Negro and Farina (2011)).

When the EMG is measured from a set of N muscles and properly demodulated, it can be empirically demonstrated that the dimensionality of the multi-muscle recording in complex tasks is smaller than the number of active muscles (figure 1) (D'Avella *et al* 2003, Mussa-Ivaldi *et al* 1994). This leads to an instantaneous linear mixture model of NM demodulated EMG channels (note that in a typical experimental setup for this type of analysis, $M = 1$ EMG channel per muscle is used):

$$z(t) \approx \mathbf{B}\mathbf{A}\lambda(t), \tag{5}$$

where $\boldsymbol{z}(t)=[z_1(t),\ldots, z_{NM}(t)]^{\mathrm{T}}$ is a vector of NM demodulated EMG channels (either by RMS or ARV metric), $\boldsymbol{\lambda}(t)=[\lambda_1(t),\ldots, \lambda_P(t)]^{\mathrm{T}}$ with $P \leq NM$ is a vector of activation primitives that drive these muscles, $\mathbf{B}$ is a $NM \times N$ crosstalk mixing matrix defined in previous subsection that denotes the signal attenuation due to volume conduction, and $\mathbf{A}$ denotes the $N \times P$ synergy matrix (figure 1):

$$\mathbf{A} = \begin{bmatrix} a_{1,1} & \cdots & a_{1,P} \\ \vdots & \ddots & \vdots \\ a_{N,1} & \cdots & a_{N,P} \end{bmatrix}. \tag{6}$$

The mixing coefficients $a_{i,p}$ determine the portion of muscle excitation by individual activation primitives and are also referred to as muscle synergies, muscle weights, or muscle modules.

According to model (5) and figure 1, muscles are not activated independently but in fixed proportions with respect to synergistic muscles. These proportions are directly reflected by the weights in the mixing matrix $\mathbf{A}$. The existence of these linear instantaneous synergistic weights (5) has been empirically validated in some conditions by showing that the dimensionality of the factorization of NM demodulated EMG signals from the forearm does not depend on the number M of EMG recording sites (Muceli *et al* 2014). However, in the presence of crosstalk the mixing matrix $\mathbf{A}$ in (5) is multiplied by the crosstalk matrix $\mathbf{B}$. The latter can be interpreted as a volume

conductor matrix that describes all the transformations of the motor unit action potential shapes depending on the fiber positions in relation to the detecting electrodes. This hinders the direct estimation of the muscles synergies (i.e. the mixing matrix **A**) from the data model (5) (Muceli *et al* 2014). It is important to notice that in this case, the crosstalk does not change the activation primitives $\boldsymbol{\lambda}(t)=[\lambda_1(t),\ldots,\lambda_P(t)]^T$ (Muceli *et al* 2014).

3. Source identification from the surface electromyogram

Methods for source separation of instantaneous mixtures, such as those in equations (4) and (5), and convolutive mixtures, such as that in (1), have been intensively studied for the past two decades and many solutions exist. Their common goal is to estimate the sources and/or the mixing matrix from the given measurements only. Ideally, as little as possible *a priori* information on the properties of the sources or mixing process should be inferred. In practice, however, a subset of the following assumptions is always used when designing a decomposition methodology (Cichocki and Amari 2002, Hyvärinen *et al* 2001).

(A1) The mixing process is stationary, so the matrices **H** in (1) and **G** and **A** in (4) and (5) do not vary over time.
(A2) The mixing matrices **H** in (1), or **G** and **A** in (4) and (5) are of full row rank and, thus, invertible i.e. the matrix inverse or at least the pseudoinverse of **G**, **A**, and **H** exists.
(A3) The sources $\mathbf{s}(t)$ in (1) are sparse i.e. the minimal interspike interval is larger than the duration of the MUAPs.
(A4) The sources $\mathbf{s}(t)$ in (1), $\mathbf{x}(t)$ in (4) or $\boldsymbol{\lambda}(t)$ in (5) are spatially uncorrelated i.e. their correlation matrix is equal to the matrix identity.
(A5) The sources $\mathbf{s}(t)$ in (1) are temporally independent i.e. each MU discharge appears independently from previous discharges.
(A6) The activation primitives $\lambda_p(t)$ and the mixing coefficients a_{ip} in (5) are nonnegative.

The assumption (A1) implies stationary conditions of the addressed mixing processes. For example, for the data model (1), it requires isometric measurements without substantial myoelectric manifestation of muscle fatigue in the observed time interval. In the case of data model (5), the assumption (A2) implies that no pair of muscles shares the same (up to a scalar factor) set of weighting coefficients for all activation primitives. In the case of data model (1), it implies that no pair of MUs with exactly the same MUAP shapes on all the channels exists, demonstrating the need for high-density surface EMG. The assumption (A4) implies that the muscle excitation patterns share no mutual information in the observed time interval (in the case of model (5)) or that no significant synchronization among the active MUs exists (in the case of models (1) and (4)). This assumption is clearly violated in several skeletal muscles (De Luca *et al* 1993), especially in the case of severe physiological or pathological tremor (Holobar *et al* 2012). The assumption (A5) derives from methodological limitations of the ICA-based source separation techniques and is not well-founded in the field of EMG, as both MUAP trains and motor neuron spike trains exhibit at least partially depended time structure. The assumption (A6) is not problematic and is guaranteed by the definition of the data model (5). The validity and further implications of these assumptions are discussed in the following subsections.

3.1. Identification of muscle synergies and activation primitives

With both activation primitives $\lambda_p(t)$ and mixing coefficients a_{ip} nonnegative (assumption (A6)), the nonnegative matrix factorization (NMF) algorithm (Lee and Seung 2001) has been

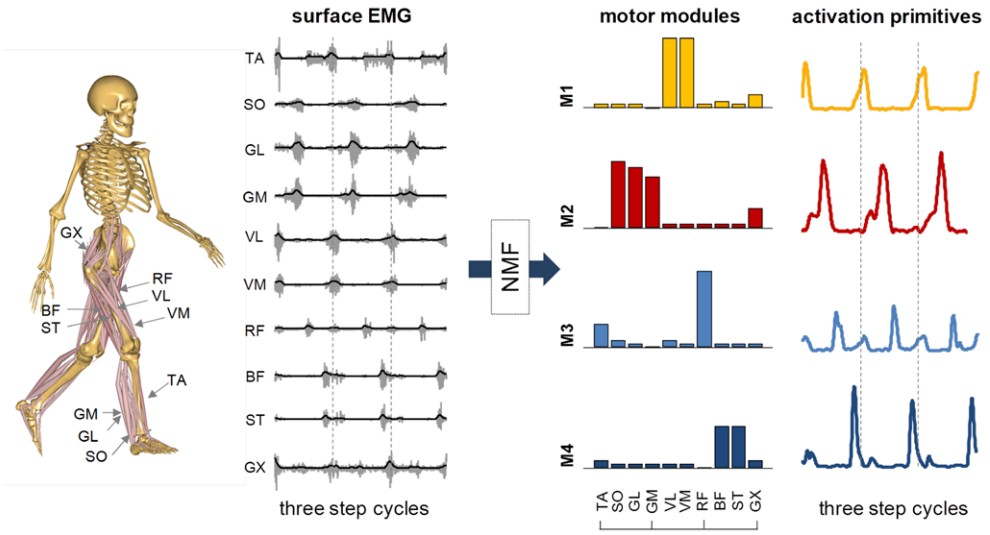

Figure 6. Factorization of human walking by NMF. The EMGs from 10 muscles have been recorded during walking at self-selected speed. The signals have been demodulated by extracting the signal envelope (black solid line) and factorized with NMF with dimensionality 4. The factorization produced muscle synergies, which are vectors of relative weights for each muscle, and in activation primitives that act on each synergy vector. The activation primitives have a periodic structure, as expected from walking, and are made of impulses of activity that determine the excitation of muscle groups in correspondence of the gait events. TA: tibialis anterior; SO: soleus; GL: gastrocnemius lateralis; GM: gastrocnemius medialis; VL: vastus lateralis; VM: vastus medialis; RF: rectus femoris; BF: biceps femoris; ST: semitendinosus; GX: gluteus maximus.

frequently applied to invert the data model (5) and estimate the common patterns in the neural drive to a group of functionally coupled muscles (D'Avella *et al* 2006, 2008, Overduin *et al* 2008, Tresch *et al* 2006). Although inferior to nonlinear demodulators, such as artificial neural networks (ANN), the NMF algorithm is nonparametric, efficient and applicable without any prior training or calibration (Jiang *et al* 2014). It relies on a relatively small number of recorded EMG channels as, typically, only one bipolar channel per muscle is recorded. Being based on minimally supervised learning, it is also relatively robust to the repositioning of the electrodes (Muceli *et al* 2014). The factorization of the demodulated EMG signal is fully nonparametric and unsupervised. The only step that requires the end user's supervision is to reorder and rescale the extracted signal components. Indeed, because of the well documented ICA-ambiguities on the energy and order of components (Cichocki and Amari 2002, Hyvärinen *et al* 2001), the extracted signal components can appear in a random order whereas their energy is typically normalized to 1.

A representative example of NMF result is presented in figure 6. In this example, the human locomotion has been investigated in a healthy man by measuring the EMG activity from 10 muscles of the lower limb. The recorded and demodulated EMG signals have been factorized and reduced in dimension to 4 activation primitives which, multiplied by the extracted synergy matrix, explained >95% of the demodulated multi-muscle signal variance. The data have been recorded during human locomotion at walking speed (self-selected by the subject). It has to be noted that the factorization identifies a peculiar structure of the activation primitives which are impulses centered at specific time instants during the gait cycle and periodically repeating over time. This burst-like excitations of muscles has been identified as a robust characteristic of human

locomotion and has been documented in walking (Lacquaniti *et al* 2012), running (Ivanenko *et al* 2007), cutting maneuvers (Oliveira *et al* 2013), as well as during robot-aided walking (Gizzi *et al* 2012, Moreno *et al* 2013). The bursts of excitation can be interpreted as central pattern generators that act on groups of muscles at times associated to different phases of the locomotion.

3.2. Reduction of EMG crosstalk

As explained in subsection 2.3, crosstalk can be described with a linear instantaneous mixture only in restricted conditions. In more general conditions, the mixture model does not apply anymore to the muscle level but to the motor unit level, presented in subsection 2.2. Conditions in which crosstalk has been treated successfully with linear mixture models are those of several, closely spaced muscles in which it is impossible to distinguish individual compartments or muscles (Muceli *et al* 2014). In this case, each EMG signal is naturally a combination of the activities of several muscles, thus crosstalk and target muscle activity may have similar intensities at any recording sites.

An example in which crosstalk signals are indistinguishable from target muscle signals are the multi-channel EMG recordings from the forearm muscles. In this case, it is not possible to target specific muscles with surface EMG electrodes since the selectivity of the recording systems is not sufficient to separate the activities of the many closely located muscle compartments of the forearm. For this reason, synergies cannot be extracted for movements of the wrist. Recently, the hypothesis that the demodulated EMG signals recorded from the forearm could be modeled as linear instantaneous mixtures (4) has been tested (Muceli *et al* 2014). The rationale was that if both matrixes **A** and **G** in figure 1 and data model (5) represented linear instantaneous mixtures and the assumption (A6) holds, then the NMF-based factorization of any number of EMG channels would lead to the same dimensionality, corresponding to the number of activation primitives. Moreover, the estimated activation primitives would not change with varying number of channels, under the same assumption. In Muceli *et al* (2014), the activation primitives and muscle synergies have been extracted from a different number of EMG channels, ranging from 128 channels down to 8 channels, during motor tasks involving 2 degrees of freedom of the wrist. The factorization by the NMF algorithm resulted always in a dimensionality equal to 4 (i.e. twice the number of degrees of freedom). Moreover, the estimated activation primitives were similar independently on the number of channels used for their extraction, as expected for linear instantaneous mixtures. Of course, the weights depended on the number of channels and, according to the model in figure 1, represented the multiplication of the matrixes **A** and **G**. Since it is not possible to separate the two matrixes in this case, the extracted weights do not correspond anymore to synergies i.e. to weights assigned to each muscle in the combination of activation primitives, but rather express the weights to be given to a specific recording location to obtain the observed demodulated EMG from the activation primitives. Despite the loss of the meaningful physiological value of the channel weights, the activation primitives maintained the meaning of high-level, task-related, neural activations and, interestingly, were indeed well correlated with the kinematics of the two degrees of freedom investigated (Muceli *et al* 2014). For this property, such primitives can be used e.g. for the control of prostheses (Jiang *et al* 2014).

3.3. Identification of MU discharge patterns

Several attempts to decompose the surface EMG measurements based on the inversion of the instantaneous mixing model (1) have been proposed in the literature (Nakamura *et al* 2004a, 2004b). For example, Nakamura *et al* (2004a, 2004b), García *et al* (2005), Theis

and García (2006), and Jiang and Farina (2011) used a linear array of surface electrodes to record eight-channel surface EMG signals from the tibialis anterior muscles during isometric dorsiflexions ranging from 5% to 20% of the maximum voluntary contraction (MVC). The recorded signals were decomposed by the fastICA decomposition algorithm (Hyvärinen 1999), which is based on assumptions (A1), (A2), (A4), and (A5) and has been extensively used in the field of latent component analysis (Cichocki and Amari 2002, Comon and Jutten 2010, Hyvärinen *et al* 2001). In García *et al* (2005), the eight-channel bipolar surface EMG was recorded from the short head of the biceps brachii by an array of 2×8 surface electrodes oriented transversely to the direction of muscle fibers. Isometric contractions were recorded with contraction forces ranging from 5% to 60% MVC. The authors combined signal-conditioning filters with the JADE decomposition algorithm (Cardoso 1999), a well-known separation algorithm that relies on assumptions (A1), (A2), (A4) and (A5). This study was further extended in Theis and García (2006), where four algorithms, namely the JADE (Cardoso 1999), NMF (Lee and Seung 1999, 2001), sparse NFM (Hoyer 2004), and sparse component analysis (SCA) (Georgiev *et al* 2005), were mutually compared and tested against their capability of separating the MUAP trains of the short head of the biceps brachii during 30% MVC isometric contractions. Although demonstrating the increase in sparseness of the identified components compared to the raw EMG signals, these studies failed to separate the contributions of individual MUs (Theis and Garcia 2006).

The reason for the failure of classic blind separation methods for linear mixtures lies in the limitations of the instantaneous data model (1) itself. First of all, the request for linear array results in rather low number of EMG channels recorded from the investigated muscle. Second, determination of the exact orientation of the muscle fibers and, thus, the positioning of the linear array is problematic. Third, even with the linear array perpendicular with respect to parallel muscle fibers, the low-pass filtering effect of the volume conductor modifies the shapes of the MUAPs beyond the effect of a simple scalar multiplication, especially at longer distances between the muscle and the uptake electrodes. This is demonstrated in figure 7, which reports the results of a simulation study and shows that even with the detection array transversal to ideally parallel muscle fibers, the average error made by the instantaneous data model (1) surpasses the average difference between the MUAP shapes of different MUs. Similar results have been demonstrated for MUs of different sizes and different positions within the muscle. Thus, methods that use the instantaneous data model (1) introduce approximations that violate assumption (A2), with consequent failure in the separation of individual MUs.

The second option for MU identification from EMG is to use the convolutive mixing model, introduced by equations (1) and (2). As mentioned in section 2.2, the convolutive model significantly increases the number of active sources, but this can be compensated by further extending the vector of measurements $\mathbf{EMG}(t)$ by K delayed repetitions of each recorded EMG channel (Holobar and Zazula 2004), with K typically ranging from 5 to 15. It was shown in Holobar and Zazula (2007a) that, after this mathematical trick, the mixing matrix $\mathbf{H}$ in (1) still combines all the MUAPs, whatever their shape. Thus, the extended convolutive model (1) still facilitates the use of two-dimensional arrays of surface electrodes. Such a model also allows the decomposition of EMG signals of pennate muscles, such as calf and hamstring muscles (Marateb *et al* 2011), which exhibit highly complex MUAP shapes when measured at the surface of the skin.

With the use of high-density EMG grids of electrodes (Merletti and Parker 2004), the number of concurrently acquired EMG channels increases to several tens. Consequently, when K delayed repetitions of each surface EMG channel are added to the vector of measurements $\mathbf{EMG}(t)$ in (1), the size of the mixing matrix $\mathbf{H}$ increases to the order of several hundreds. As a result, hardly any decomposition method aims at estimating the whole mixing matrix. Instead,

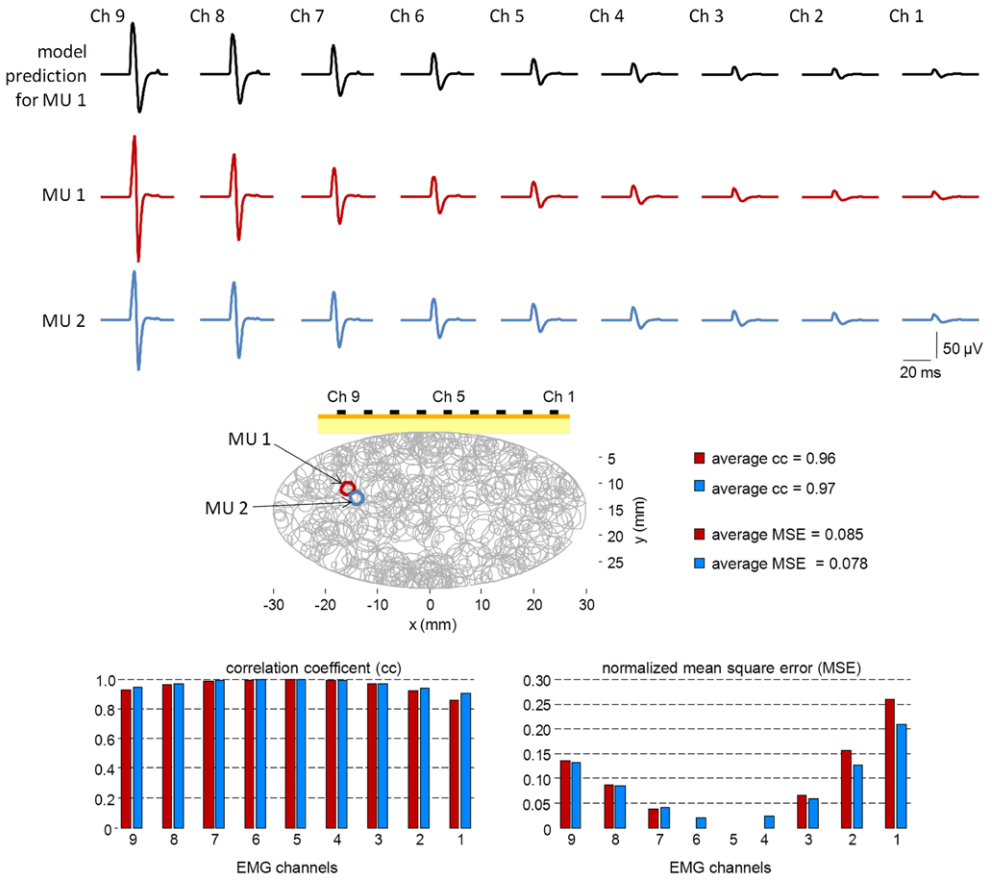

Figure 7. The MUAP shapes as predicted by the instantaneous mixing model (black) and the actual MUAP shapes (red) as detected by nine uptake electrodes for a MU 1 whose territory is indicated by the red thick line in the central panel. For a comparison, the MUAP shapes of a nearby MU 2 (indicated by the blue thick line in the central panel) are also depicted in blue. The lower panel reports the matching between the predicted and actual MUAP shapes of MU 1 (red) and the difference between the MUAP shapes of MUs 1 and 2 (blue). The error made by the instantaneous mixing model (1) is greater than the differences between the MUAP shapes of the MUs 1 and 2. The synthetic surface EMG signals were generated by the multilayer cylindrical volume conductor model proposed in Farina *et al* (2004c).

the discharge patterns of individual MU discharges are assessed sequentially, one after the other (Holobar and Zazula 2004, 2007a).

A very effective sequential MU identification technique, so called convolution kernel compensation (CKC) approach, was proposed by Holobar and Zazula (2004, 2007a). This method builds on assumptions (A1), (A2), and (A3) and directly estimates the MU discharge patterns, without estimating the mixing matrix **H** in (1). Up to now, two different CKC-based approaches to MU identification have been proposed. In Holobar and Zazula (2007a), the sequential probabilistic approach was introduced. This approach still requires assumption (A4) to hold. A more efficient approach has been proposed in Holobar and Zazula (2007b), where a gradient optimization of the non-linear cost function of the estimated MU discharge pattern has been used to iteratively improve the MU identification. The gradient based optimization has been proven to converge also in the case of highly synchronized MU discharge

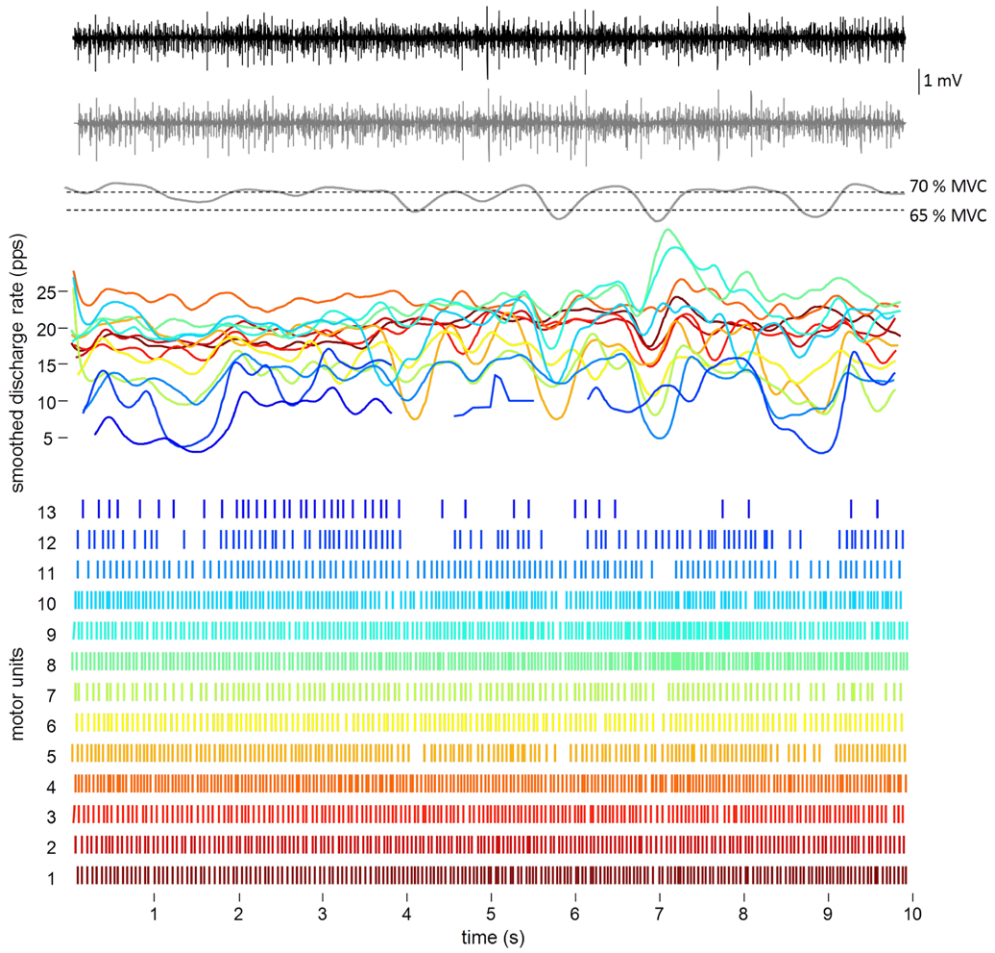

Figure 8. MU discharge patterns as identified by a gradient CKC decomposition routine from the high-density EMG of biceps brachii muscle of a young healthy male, during its 70% MVC contraction. Each vertical line in the lower panel represents one MU discharge. The central panel depicts the smoothed discharge rates of identified MUs along with the smoothed muscle force (low-pass Butterworth filter, cut-off frequency of 2 Hz). The upper panel shows the raw EMG channel in bipolar configuration (black) and the corresponding sum of identified MUAP trains (gray). High accuracy (>90%) of the identified MU discharge patterns has been validated by the signal-based methodology presented in Holobar *et al* (2014).

patterns (Holobar *et al* 2012), abolishing the need for assumption (A4). This is of paramount importance when studying the MU discharge patterns in the case of physiological or pathological tremor (Benito-León and Louis 2006, Brittain and Brown 2013). In the last decade, this technique has been extensively validated (for details, see Holobar and Zazula 2004, Holobar and Zazula 2007a, Holobar *et al* 2009, 2010, 2012, Marateb *et al* 2011). In addition, a highly-efficient signal-based measure of accuracy of every identified MU has been proposed and systematically validated in Holobar *et al* (2014).

Figure 8 presents the results of MU identification from the surface EMG of the biceps brachii muscle of a healthy young man. The surface EMG signals were acquired with a 9×10 matrix of surface electrodes (LISiN, Politecnico di Torino, Italy), with interelectrode distance

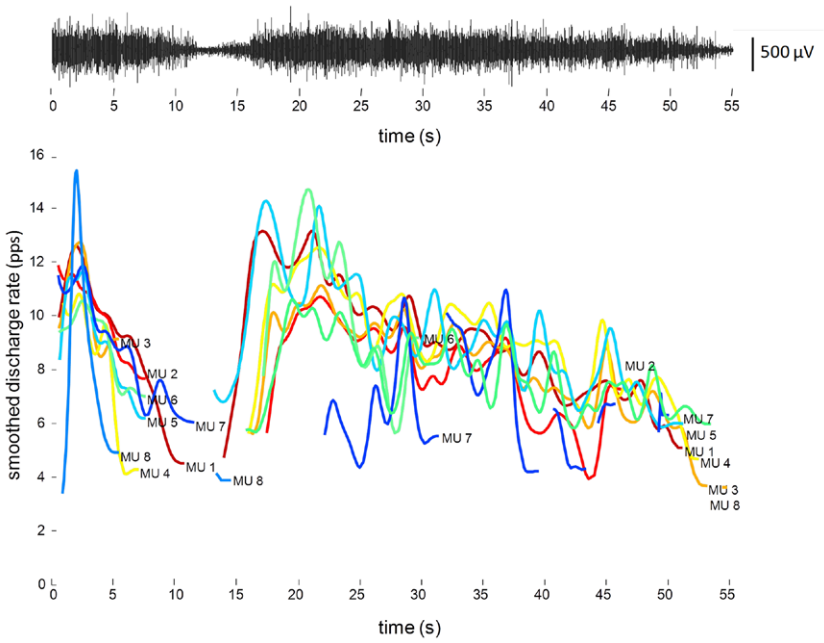

Figure 9. Smoothed discharge rates of MUs identified from a surface EMG of abductor hallucis muscle during cramp elicited with electrical stimulation of the muscle motor point. The EMG signals were acquired by a 6×5 grid of electrodes (2 mm diameter, 5 mm inter-electrode distance; LISiN, Politecnico di Torino, Italy) placed between the muscle motor point and the distal tendon and decomposed by CKC decomposition method. Cramp was elicited by electrical stimulation (Minetto *et al* 2007) and extinguished spontaneously in the first 10 s after the end of stimulation but reappeared 15 s after the end of stimulation. Time 0 corresponds to the end of electrical stimulation.

of 5 mm, during an isometric muscle contraction at 70% of MVC. The discharge patterns and smoothed discharge rates of the identified MUs are depicted, along with the smoothed exerted muscle force. The smoothing was performed by a second order Butterworth filter with cut-off frequency of 2 Hz. The raw EMG signal and the corresponding sum of identified MUAP trains are also depicted.

In isometric conditions, the CKC-based MU identification has been successfully applied to the full range of contraction forces and validated in muscles with highly diverse anatomy such as calf, quadriceps and hamstring muscles (Holobar *et al* 2010, Marateb *et al* 2011), shoulder and arm muscles (Holobar *et al* 2009, 2010), wrist and finger muscles (Holobar *et al* 2010, 2012), facial muscles (Radeke *et al* 2014), and anal sphincters (Cescon *et al* 2011). They have also been validated in patients with neurodegenerative diseases, such as essential and Parkinsonian tremor that cause high degree of MU synchronization (Holobar *et al* 2012), in type II diabetes patients (Watanabe *et al* 2013) and cleft lip patients (Radeke *et al* 2014).

The application of surface EMG decomposition into individual MU spike trains is particularly relevant in conditions where the use of invasive electrodes, as alternative to MU analysis, is complicated by experimental constraints. For example, figure 9 reports the decomposition of surface EMG signals during a muscle cramp. Despite the highly complex interferential patterns in the surface EMG, this result of the fully automatic decomposition agreed almost perfectly with the results of EMGlab-based decomposition (McGill *et al* 2005) of concurrently

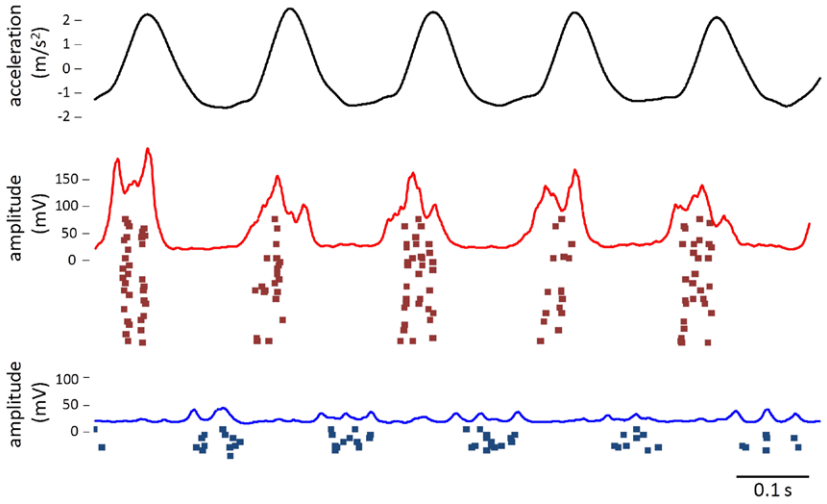

Figure 10. Pathological tremor in an ET patient with a severe tremor as measured by an inertial measuring unit mounted at the third metacarpal of the patient's dominant hand (top panel), rectified surface EMG from wrist extensors (central panel), and from wrist flexors (bottom panel) during the arms outstretched task. MU discharge patterns as identified by gradient CKC method from the extensors and flexors are depicted by red and blue dots (central and bottom), respectively. Each dot represents one MU discharge. A strong MU synchronization in extensor is clearly visible. High accuracy (>95%) of the identified MU discharge patterns has been validated by the signal-based methodology presented in Holobar *et al* (2014).

acquired intramuscular EMG (Minetto *et al* 2013). The behavior of the identified MUs show a correlated activity, which underlines sources of common drive to the motor neurons during cramp contractions (Minetto *et al* 2013).

The latest developments in the surface EMG decomposition enabled non-invasive, frequent and long-term identification of MU discharge patterns, even at extremely high levels of MU synchronization, such as in the case of pathological tremor (Holobar *et al* 2012). Figure 10 depicts the decomposition of EMG signals recorded from the wrist extensor and flexor muscles in an essential tremor patient with a severe tremor. For clarity reasons, the rectified surface EMG and the accelerations of the wrist as measured by inertial measuring unit are also depicted. The pathological synchronizations and paired discharges of a relatively large number of MUs are clearly visible in the wrist extensors. The tremor in the wrist flexors is less pronounced and MU synchronization is significantly lower than in the wrist extensors.

4. Conclusions

The surface EMG reflects the output spike trains of the alpha motor neurons. Because the alpha motor neurons receive synaptic input from the entire neuromuscular system and generate the neural excitation signals to the skeletal muscles, the surface EMG contains neural information at different levels. The demodulated surface EMG signals to the muscles involved in complex tasks are determined by activation primitives that are believed to be generated at the supraspinal level. When recording from individual muscles, however, the EMG not only represents the activity of the target muscle but also that of nearby muscles, because of volume conduction. Finally, the electrical activity of each individual muscle can be seen as the convolutive mixture

of the spike trains of the active motor neurons. These mixing processes, at different levels of neural excitation, can be identified relatively accurately by currently available blind source separation techniques that assume as little *a priori* information on the mixing process as possible. In the last decade, these techniques have been under intense development and validation, especially for the identification of individual MUs, and have demonstrated remarkable results. Thus, despite not being a signal recorded from neural cells directly, the surface EMG allows detailed and noninvasive investigations of the neural control of movement. The needed number of EMG channels depends on the application. High-density surface EMG is required for the identification of individual motor units, whereas reduction of crosstalk and assessment of activation primitives can be performed even with only one recording per muscle.

Acknowledgments

This study was supported by the Commission of the European Union, within Framework 7, under Grant Agreement number ICT-2011.5.1-287739 'NeuroTREMOR: A novel concept for support to diagnosis and remote management of tremor' (AH), by Slovenian Research Agency (contract #L5-5550: Definition of non-invasive marker for skeletal muscle atrophy: from validation to application) (AH) and the European Research Council Advanced Grant DEMOVE (contract #267888) (DF).

References

Benito-León J and Louis E D 2006 Essential tremor: emerging views of a common disorder *Nat. Clin. Pract. Neurol.* **2** 666–78

Bernstein N A 1967 *The Co-Ordination and Regulation of Movements* (New York: Pergamon)

Blok J H, Van Dijk J P, Zwarts M J and Stegeman D F 2005 Motor unit action potential topography and its use in motor unit number estimation *Muscle Nerve* **32** 280–91

Brittain J S and Brown P 2013 The many roads to tremor *Exp. Neurol.* **250C** 104–7

Cardoso J F 1999 High-order contrasts for independent component analysis *Neural Comput.* **11** 157–92

Cescon C, Mesin L, Nowakowski M and Merletti R 2011 Geometry assessment of anal sphincter muscle based on monopolar multichannel surface EMG signals *J. Electromyogr. Kinesiol.* **21** 394–401

Cichocki A and Amari S 2002 *Adaptive Blind Signal and Image Processing* 1st edn (Chichester: Wiley)

Clancy E A and Hogan N 1999 Probability density of the surface electromyogram and its relation to amplitude detectors *IEEE Trans. Biomed. Eng.* **46** 730–9

Comon P and Jutten C 2010 *Handbook of Blind Source Separation Independent Component Analysis and Blind Deconvolution* (Oxford: Academic)

D'Avella A, Fernandez L, Portone A and Lacquaniti F 2008 Modulation of phasic and tonic muscle synergies with reaching direction and speed *J. Neurophysiol.* **100** 1433–54

D'Avella A, Portone A, Fernandez L and Lacquaniti F 2006 Control of fast-reaching movements by muscle synergy combinations *J. Neurosci.* **26** 7791–810

D'Avella A, Saltiel P and Bizzi E 2003 Combinations of muscle synergies in the construction of a natural motor behavior *Nat. Neurosci.* **6** 300–8

De Luca C J, Adam A, Wotiz R, Gilmore L D and Nawab S H 2006 Decomposition of surface EMG signals *J. Neurophysiol.* **96** 1646–57

De Luca C J, LeFever R S, McCue M P and Xenakis A P 1982 Control scheme governing concurrently active human motor units during voluntary contractions *J. Physiol. (Lond.)* **329** 129–42

De Luca C J and Merletti R 1988 Surface myoelectric signal cross-talk among muscles of the leg *Electroencephalogr. Clin. Neurophysiol.* **69** 568–75

De Luca C J, Roy A M and Erim Z 1993 Synchronization of motor-unit firings in several human muscles *J. Neurophysiol.* **70** 2010–23

Djuwari D, Kumar D K, Naik G R, Arjunan S P and Palaniswami M 2006 Limitations and applications of ICA for surface electromyogram *Electromyogr. Clin. Neurophysiol.* **46** 295–309
Evans H B, Pan Z, Parker P A and Scott R N 1984 Signal processing for proportional myoelectric control *IEEE Trans. Biomed. Eng*. **31** 207–11
Farina D and Merletti R 2001 Effect of electrode shape on spectral features of surface detected motor unit action potentials *Acta. Physiol. Pharmacol. Bulg.* **26** 63–6
Farina D and Negro F 2012 Accessing the neural drive to muscle and translation to neurorehabilitation technologies *IEEE Rev. Biomed. Eng*. **5** 3–14
Farina D and Rainoldi A 1999 Compensation of the effect of sub-cutaneous tissue layers on surface EMG: a simulation study *Med. Eng. Phys*. **21** 487–97
Farina D, Cescon C and Merletti R 2002 Influence of anatomical, physical, and detection-system parameters on surface EMG *Biol. Cybern.* **86** 445–56
Farina D, Févotte C, Doncarli C and Merletti R 2004a Blind separation of linear instantaneous mixtures of nonstationary surface myoelectric signals *IEEE Trans. Biomed. Eng.* **51** 1555–67
Farina D, Gazzoni M and Camelia F 2004b Low-threshold motor unit membrane properties vary with contraction intensity during sustained activation with surface EMG visual feedback *J. Appl. Physiol*. **96** 1505–15
Farina D, Holobar A, Merletti R and Enoka R M 2010 Decoding the neural drive to muscles from the surface electromyogram *Clin. Neurophysiol.* **121** 1616–23
Farina D, Lucas M F and Doncarli C 2008 Optimized wavelets for blind separation of nonstationary surface myoelectric signals *IEEE Trans. Biomed. Eng.* **55** 78–86
Farina D, Mesin L, Martina S and Merletti R 2004c A surface EMG generation model with multilayer cylindrical description of the volume conductor *IEEE Trans. Biomed. Eng.* **51** 415–26
Farina D, Negro F and Jiang N 2013 Identification of common synaptic inputs to motor neurons from the rectified electromyogram *J. Physiol.* **591** 2403–18
Fuglevand A J, Winter D A and Patla A E 1993 Models of recruitment and rate coding organization in motor-unit pools *J. Neurophysiol.* **70** 2470–88
García G A, Okuno R and Akazawa K 2005 A decomposition algorithm for surface electrode-array electromyogram. A noninvasive, three-step approach to analyze surface EMG signals *IEEE Eng. Med. Biol. Mag.* **24** 63–72
Georgiev P, Theis F and Cichocki A 2005 Sparse component analysis and blind source separation of underdetermined mixtures *IEEE Trans. Neural Netw.* **16** 992–6
Gizzi L, Nielsen J F, Felici F, Ivanenko Y P and Farina D 2011 Impulses of activation but not motor modules are preserved in the locomotion of subacute stroke patients *J. Neurophysiol.* **106** 202–10
Gizzi L, Nielsen J F, Felici F, Moreno J C, Pons J L and Farina D 2012 Motor modules in robot-aided walking *J. Neuroeng. Rehabil.* **9** 76
Gosselin B 2011 Recent advances in neural recording microsystems *Sensors (Basel)* **11** 4572–97
Hannan M A, Abbas S M, Samad S A and Hussain A 2012 Modulation techniques for biomedical implanted devices and their challenges *Sensors (Basel)* **12** 297–319
Hogan N and Mann R W 1980 Myoelectric signal processing: optimal estimation applied to electromyography—part I: derivation of the optimal myoprocessor *IEEE Trans. Biomed. Eng.* **27** 382–95
Holobar A and Zazula D 2004 Correlation-based decomposition of surface electromyograms at low contraction forces *Med. Biol. Eng. Comput.* **42** 487–95
Holobar A and Zazula D 2007a Multichannel blind source separation using convolution kernel compensation *IEEE Trans. Signal Process.* **55** 4487–96
Holobar A and Zazula D 2007b Gradient convolution kernel compensation applied to surface electromyograms *Lect. Notes Comput. Sci.* **4666** 617–24
Holobar A, Farina D, Gazzoni M, Merletti R and Zazula D 2009 Estimating motor unit discharge patterns from high-density surface electromyogram *Clin. Neurophysiol.* **120** 551–62
Holobar A, Glaser V, Gallego J A, Dideriksen J L and Farina D 2012 Non-invasive characterization of motor unit behaviour in pathological tremor *J. Neural. Eng.* **9** 056011
Holobar A, Minetto M A and Farina D 2014 Accurate identification of motor unit discharge patterns from high-density surface EMG and validation with a novel signal-based performance metric *J. Neural Eng*. **11** 016008
Holobar A, Minetto M A, Botter A, Negro F and Farina D 2010 Experimental analysis of accuracy in the identification of motor unit spike trains from high-density surface EMG *IEEE Trans. Neural. Syst. Rehabil. Eng.* **18** 221–9

Hoyer P 2004 Non-negative matrix factorization with sparseness constraints *J. Mach. Learn. Res.* **5** 1457–69
Hyvärinen A 1999 Fast and robust fixed-point algorithms for independent component analysis *IEEE Trans. Neural Netw.* **10** 626–34
Hyvärinen A, Karhunen J and Oja E 2001 *Independent Component Analysis* (New York: Wiley-Interscience) pp 147–64
Ivanenko Y P, Cappellini G, Dominici N, Poppele R E and Lacquaniti F 2007 Modular control of limb movements during human locomotion *J. Neurosci*. **27** 11149–61
Ivanenko Y P, Poppele R E and Lacquaniti F 2004 Five basic muscle activation patterns account for muscle activity during human locomotion *J. Physiol. (Lond.)* **556** 267–82
Jensen M B, Manresa J A B, Frahm K S and Andersen O K 2013 Analysis of muscle fiber conduction velocity enables reliable detection of surface EMG crosstalk during detection of nociceptive withdrawal reflexes. *BMC Neurosci.* **14** 39
Jiang N and Farina D 2011 Covariance and time-scale methods for blind separation of delayed sources *IEEE Trans. Biomed. Eng.* **58** 550–6
Jiang N, Englehart K B and Parker P A 2009 Extracting simultaneous and proportional neural control information for multiple-DOF prostheses from the surface electromyographic signal *IEEE Trans. Biomed. Eng.* **56** 1070–80
Jiang N, Rehbaum H, Vujaklija I, Graimann B and Farina D 2014 Intuitive, online, simultaneous and proportional myoelectric control over two degrees of freedom in upper limb amputees *IEEE Trans. Neural. Syst. Rehabil. Eng.* **22** 501–10
Jiang N, Vest-Nielsen J L G, Muceli S and Farina D 2012 EMG-based simultaneous and proportional estimation of wrist/hand kinematics in uni-lateral trans-radial amputees *J. Neuroeng. Rehabil*. **9** 42
Kuiken T A, Li G, Lock B A, Lipschutz R D, Miller L A, Stubblefield K A and Englehart K B 2009 Targeted muscle reinnervation for real-time myoelectric control of multifunction artificial arms *JAMA* **301** 619–28
Lacquaniti F, Ivanenko Y P and Zago M 2012 Patterned control of human locomotion *J. Physiol.* **590** 2189–99
Lee D D and Seung H S 1999 Learning the parts of objects by non-negative matrix factorization *Nature* **401** 788–91
Lee D D and Seung H S 2001 Algorithms for non-negative matrix factorization *Adv. Neural Inf. Process. Syst.* **13** 556–62
Léouffre M, Quaine F and Servière C 2013 Testing of instantaneity hypothesis for blind source separation of extensor indicis and extensor digiti minimi surface electromyograms *J. Electromyogr. Kinesiol.* **23** 908–15
Lindstrom L H and Magnusson R I 1977 Interpretation of myoelectric power spectra: a model and its applications *Proc. IEEE* **65** 653–62
Ling S M, Conwit R A, Talbot L, Shermack M, Wood J E, Dredge E M, Weeks M J, Abernethy D R and Metter E J 2007 Electromyographic patterns suggest changes in motor unit physiology associated with early osteoarthritis of the knee *Osteoarthr. Cartil.* **15** 1134–40
Lorrain T, Jiang N and Farina D 2011 Influence of the training set on the accuracy of surface EMG classification in dynamic contractions for the control of multifunction prostheses *J. Neuroeng. Rehabil*. **8** 25
Marateb H R, McGill K C, Holobar A, Lateva Z C, Mansourian M and Merletti R 2011 Accuracy assessment of CKC high-density surface EMG decomposition in biceps femoris muscle *J. Neural. Eng.* **8** 066002
McGill K C, Lateva Z C and Marateb H R 2005 EMGLAB: an interactive EMG decomposition program *J. Neurosci. Methods*. **149** 121–33
Meigal A Y, Rissanen S M, Tarvainen M P, Airaksinen O, Kankaanpää M and Karjalainen P A 2013 Non-linear EMG parameters for differential and early diagnostics of Parkinson's disease *Front. Neurol*. **4** 135
Merletti R and Parker P J 2004 *Electromyography: Physiology, Engineering, and Non-Invasive Applications* (Piscataway, NJ: IEEE)
Merletti R, Aventaggiato M, Botter A, Holobar A, Marateb H and Vieira T M M 2010 Advances in surface EMG: recent progress in detection and processing techniques *Crit. Rev. Biomed. Eng.* **38** 305–45
Minetto M A, Holobar A, Botter A and Farina D 2013 Origin and development of muscle cramps *Exerc. Sport. Sci. Rev.* **41** 3–10

Minetto M A, Rainoldi A and Jabre J F 2007 The clinical use of macro and surface electromyography in diagnosis and follow-up of endocrine and drug-induced myopathies *J. Endocrinol. Invest.* **30** 791–6

Moreno J C, Barroso F, Farina D, Gizzi L, Santos C, Molinari M and Pons J L 2013 Effects of robotic guidance on the coordination of locomotion *J. Neuroeng. Rehabil.* **10** 79

Muceli S and Farina D 2012 Simultaneous and proportional estimation of hand kinematics from EMG during mirrored movements at multiple degrees-of-freedom *IEEE Trans. Neural. Syst. Rehabil. Eng*. **20** 371–8

Muceli S, Boye A T, D'Avella A and Farina D 2010 Identifying representative synergy matrices for describing muscular activation patterns during multidirectional reaching in the horizontal plane *J. Neurophysiol.* **103** 1532–42

Muceli S, Jiang N and Farina D 2014 Extracting signals robust to electrode number and shift for online simultaneous and proportional myoelectric control by factorization algorithms *IEEE Trans. Neural. Syst. Rehabil. Eng.* **22** 623–33

Mussa-Ivaldi F A, Giszter S F and Bizzi E 1994 Linear combinations of primitives in vertebrate motor control *Proc. Natl Acad. Sci. USA* **91** 7534–8

Naik G R and Kumar D K 2012 Identification of hand and finger movements using multi run ICA of surface electromyogram *J. Med. Syst.* **36** 841–51

Naik G R, Arjunan S and Kumar D 2011 Applications of ICA and fractal dimension in sEMG signal processing for subtle movement analysis: a review *Australas. Phys. Eng. Sci. Med.* **34** 179–93

Naik G R, Kumar D K and Palaniswami M 2008 Surface EMG based hand gesture identification using semi blind ICA: validation of ICA matrix analysis *Electromyogr. Clin. Neurophysiol*. **48** 169–80

Nakamura H, Yoshida M, Kotani M, Akazawa K and Moritani T 2004a The application of independent component analysis to the multi-channel surface electromyographic signals for separation of motor unit action potential trains: part I-measuring techniques *J. Electromyogr. Kinesiol*. **14** 423–32

Nakamura H, Yoshida M, Kotani M, Akazawa K and Moritani T 2004b The application of independent component analysis to the multi-channel surface electromyographic signals for separation of motor unit action potential trains: part II-modelling interpretation *J. Electromyogr. Kinesiol*. **14** 433–41

Nawab S H, Chang S S and De Luca C J 2010 High-yield decomposition of surface EMG signals *Clin. Neurophysiol.* **121** 1602–15

Neblett R, Brede E, Mayer T G and Gatchel R J 2013 What is the best surface EMG measure of lumbar flexion-relaxation for distinguishing chronic low back pain patients from pain-free controls? *Clin. J. Pain* **29** 334–40

Negro F and Farina D 2011 Linear transmission of cortical oscillations to the neural drive to muscles is mediated by common projections to populations of motoneurons in humans *J. Physiol*. **589** 629–37

Oliveira A S, Silva P B, Lund M E, Kersting U G and Farina D 2013 Fast changes in direction during human locomotion are executed by impulsive activation of motor modules *Neuroscience* **228** 283–93

Overduin S A, D'Avella A, Roh J and Bizzi E 2008 Modulation of muscle synergy recruitment in primate grasping *J. Neurosci.* **28** 880–92

Pantall A, Durham S and Ewins D 2011 Surface electromyographic activity of five residual limb muscles recorded during isometric contraction in transfemoral amputees with osseointegrated prostheses *Clin. Biomech.* **26** 760–5

Raasch C C and Zajac F E 1999 Locomotor strategy for pedaling: muscle groups and biomechanical functions *J. Neurophysiol.* **82** 515–25

Radeke J, van Dijk J P, Holobar A and Lapatki B G 2014 Electrophysiological method for examining the muscle fiber architecture of the upper lip in cleft-lip subjects, *J. Orofac. Orthop.* **75** 51–61

Richard P D, Gander R E, Parker P A and Scott R N 1983 Multistate myoelectric control: the feasibility of 5-state control *J. Rehabil. Res. Dev.* **20** 84–6

Roeleveld K, Stegeman D F, Falck B and Stålberg E V 1997a Motor unit size estimation: confrontation of surface EMG with macro EMG *Electroencephalogr. Clin. Neurophysiol.* **105** 181–8

Roeleveld K, Stegeman D F, Vingerhoets H M and Van Oosterom A 1997b The motor unit potential distribution over the skin surface and its use in estimating the motor unit location *Acta Physiol. Scand.* **161** 465–72

Roh J, Rymer W Z and Beer R F 2012 Robustness of muscle synergies underlying three-dimensional force generation at the hand in healthy humans *J. Neurophysiol*. **107** 2123–42
Sanger T D 2008 Use of surface electromyography (EMG) in the diagnosis of childhood hypertonia: a pilot study *J. Child. Neurol.* **23** 644–8
Sartori M, Gizzi L, Lloyd D G and Farina D 2013 A musculoskeletal model of human locomotion driven by a low dimensional set of impulsive excitation primitives *Front. Comput. Neurosci.* **7** 79
Staudenmann D, Daffertshofer A, Kingma I, Stegeman D F and van Dieën J H 2007 Independent component analysis of high-density electromyography in muscle force estimation *IEEE Trans. Biomed. Eng.* **54** 751–4
Theis F J and García G A 2006 On the use of sparse signal decomposition in the analysis of multi-channel surface electromyograms *Signal Process.* **86** 603–23
Ting L H and Macpherson J M 2005 A limited set of muscle synergies for force control during a postural task *J. Neurophysiol.* **93** 609–13
Torres-Oviedo G and Ting L H 2010 Subject-specific muscle synergies in human balance control are consistent across different biomechanical contexts *J. Neurophysiol.* **103** 3084–98
Torres-Oviedo G, Macpherson J M and Ting L H 2006 Muscle synergy organization is robust across a variety of postural perturbations *J. Neurophysiol.* **96** 1530–46
Tresch M C, Cheung V C and D'Avella A 2006 Matrix factorization algorithms for the identification of muscle synergies: evaluation on simulated and experimental data sets *J. Neurophysiol.* **95** 2199–212
Vaiman M and Krakovski D 2012 EMG assessment of analgesia in treatment of posttonsillectomy pain: random allocation, preliminary report *Clin. J. Pain* **28** 143–8
Watanabe K, Gazzoni M, Holobar A, Miyamoto T, Fukuda K, Merletti R and Moritani T 2013 Motor unit firing pattern of vastus lateralis muscle in type 2 diabetes mellitus patients *Muscle Nerve* **48** 806–13
Watanabe K, Miyamoto T, Tanaka Y, Fukuda K and Moritani T 2012 Type 2 diabetes mellitus patients manifest characteristic spatial EMG potential distribution pattern during sustained isometric contraction *Diabetes Res. Clin. Pract.* **97** 468–73
Woźniak K, Piątkowska D, Lipski M and Mehr K 2013 Surface electromyography in orthodontics—a literature review *Med. Sci. Monit.* **19** 416–23
Zariffa J, Steeves J and Pai D K 2012 Changes in hand muscle synergies in subjects with spinal cord injury: characterization and functional implications *J. Spinal. Cord. Med*. **35** 310–18
Zhang Q, Jonasson C and Styf J 2011 Simultaneous intramuscular pressure and surface electromyography measurement in diagnosing the chronic compartment syndrome *Scand. J. Med. Sci. Sports* **21** 190–5
Zhang X, Barkhaus P, Rymer W and Zhou P 2013 Machine learning for supporting diagnosis of *amyotrophic* lateral sclerosis using surface electromyogram *IEEE Trans. Neural. Syst. Rehabil. Eng.* **22** 96–103